

<sup>9</sup>T. Ohnuma, S. Miyake, T. Sato, and T. Watari, Phys. Rev. Lett. **26**, 541 (1971); T. Ohnuma, S. Miyake, T. Watanabe, T. Watari, and T. Sato, Phys. Rev.

Lett. **30**, 535 (1973).

<sup>10</sup>T. H. Stix, *The Theory of Plasma Waves* (McGraw-Hill, New York, 1962), p. 225.

## Observation of Two Ion-Acoustic Waves in an Argon-Helium Plasma

Y. Nakamura, M. Nakamura, and T. Itoh

*Institute of Space and Aeronautical Science, University of Tokyo, Komaba, Meguro-ku, Tokyo, Japan*

(Received 1 December 1975; revised manuscript received 5 April 1976)

The propagation of ion-acoustic waves in two-ion plasmas is investigated both experimentally and theoretically when the ratio of electron to ion temperature is 10 to 15. Although a single mode is observed in an argon-neon plasma, two modes are detected in an argon-helium plasma.

In this Letter, the propagation of linear ion-acoustic waves in a plasma which contains two species of ions is studied. Such multispecies ion plasmas are rather frequently encountered. For example, the upper ionosphere plasma consists of  $O^+$ ,  $H^+$ , and  $He^+$ ; a lithium and deuterium plasma is of thermonuclear interest.

Recently, Jones *et al.*<sup>1</sup> have observed ion-acoustic waves in a two-electron-temperature plasma. They found that a single mode propagates with an acoustic velocity calculated from the effective temperature when the electron-to-ion temperature ratio  $T_e/T_i$  was much greater than 1. On the other hand, in the two-ion plasma, the number of modes depends on  $T_e/T_i$  and the ratio of heavy-ion mass to light-ion mass.

Ion-acoustic waves, whose wave number  $K$  is much smaller than the Debye wave number  $K_e$  in a multi-ion plasma, have been studied theoretically by Fried, White, and Samec.<sup>2</sup> They examined the case of Ar-He plasma and found some new phenomena which had not been observed in a single-ion plasma. These phenomena are the following: (1) The damping rate of the wave is strongly enhanced by a small amount of light-ion contamination. The enhanced Landau damping has been already found experimentally by Alexeff, Jones, and Montgomery.<sup>3</sup> (2) When  $T_e/T_i$  is larger than about 20, the phase velocity increases from the acoustic speed of argon ions to that of helium ions with an increase in the helium-ion concentration. The wave damping rate has a maximum when  $r$  is small. It has been experimentally observed and reported in a previous paper.<sup>4</sup> (3) When  $T_e/T_i$  is smaller than 20, two modes of ion-acoustic waves coexist in a certain region of  $r$ . The purpose of this experiment is to observe whether two ion-acoustic waves coexist or

not in Ar-He and Ar-Ne plasmas under the condition of  $T_e/T_i = 10$  to 15.

The experiments were performed with a stainless-steel chamber 40 cm in diameter and 100 cm in length. Inside the chamber twelve oxide-coated cathodes 2 mm wide and 12 cm long were set at 5 cm from the wall. The plasma was created by discharge between cathodes at a negative potential of 45 V and the grounded wall. The gas pressure was 0.1 to 3.0 mTorr. The discharge current which depended on the pressure was 3 to 7 A. The plasma density was  $10^8$ – $10^9$  cm<sup>-3</sup>. The electron temperature  $T_e$  was 1.6 to 2.0 eV in the Ar-He plasma. The ion temperature  $T_i$  was measured by an energy analyzer which consisted of two grids (100 lines/in.) and a collector plate and it was 0.15 to 0.20 eV. The ion temperature was also estimated from the damping rate of the ion-acoustic wave in the pure-argon plasma and it was about 0.2 eV. As a result of this,  $T_e/T_i$  is 10 to 15.

The wave was excited by a grid 10 cm in diameter positioned at the center of the plasma chamber and was detected by a plane probe 0.5 cm in diameter which was movable along the chamber axis. The dispersion relation was obtained by the interferometer technique by launching continuous waves. The rf voltage applied to the grid was 0.5 V peak to peak. The dc potential of the grid was -20 V. The group velocity was measured by the time-of-flight technique by launching single pulses of 3  $\mu$ sec. The pulse height was 1 V. The light-ion concentration  $r$  was monitored by the ion saturation current of the energy analyzer and the electron density was measured by a Langmuir probe.<sup>4</sup>

Typical raw data from the interferometer are shown in Fig. 1 for different  $r$  of the Ar-He plas-

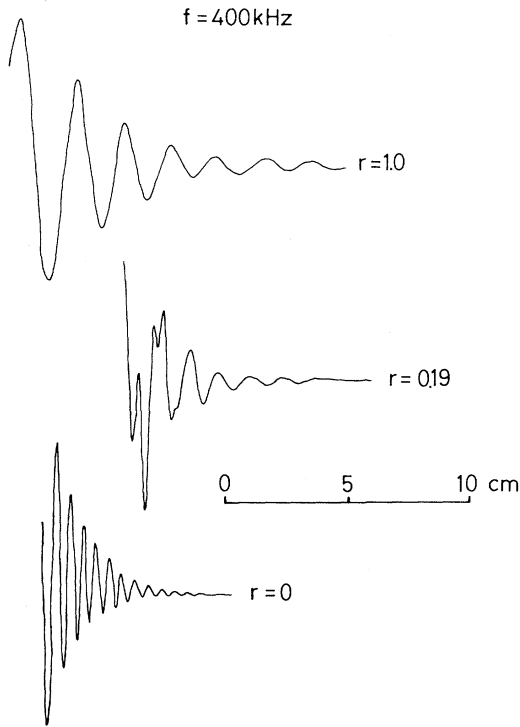


FIG. 1. Typical raw data for the wave propagations.

ma. The wave frequency is 400 kHz. As seen in the figure, when  $r=0$  (pure-argon plasma) and  $r=1$  (pure-helium plasma), a single ion acoustic wave propagates. On the other hand, when  $r=0.19$ , two modes propagate so that the wave pattern shows interference of the two waves. From the data such as shown in Fig. 1, wavelengths were estimated for different frequencies. The dispersion relation was linear in the measured frequency region and the phase velocity for  $K \ll K_e$  could be obtained. The phase velocity was equal to the group velocity measured by the time-of-flight method.

The measured phase velocities of the wave in the Ar-He plasma are shown in Fig. 2 as a function of  $r$  by closed circles. The phase velocity when  $r=0$  is shown by an arrow in the figure, which corresponds to the ion-acoustic velocity for pure-argon plasma. As the density of helium ions increases the phase velocity of the argon ion-acoustic wave decreases. This mode was observed up to  $r \approx 0.4$ . When  $r > 0.4$  it could not be detected because of its heavy damping and only the helium mode was observed. When  $0.04 \leq r \leq 0.4$ , two modes are seen to propagate. When  $r < 0.04$  it was very difficult to transmit the helium mode because of its small excitation.

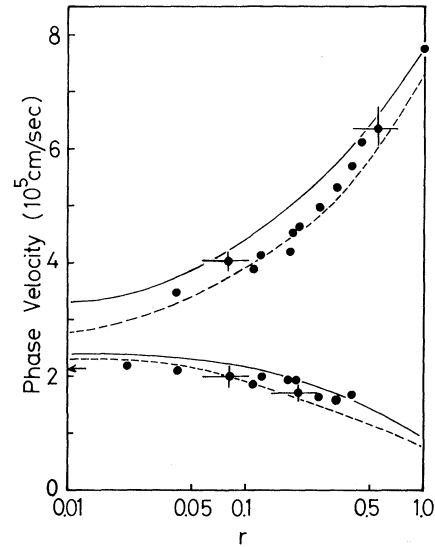


FIG. 2. Dependence of phase velocities on helium-ion concentration. The arrow shows the phase velocity at  $r=0$ . The solid and dashed lines are calculated from Eq. (1) for  $T_e/T_i=10$  and 15, respectively, where  $T_e$  is 1.8 eV.

The dispersion relation of ion-acoustic waves in the two-ion plasma is given by<sup>2</sup>

$$\frac{2K^2}{K_e^2} = Z' \left( \frac{\omega}{KV_e} \right) + \frac{T_e(1-r)}{T_h} Z' \left( \frac{\omega}{KV_h} \right) + \frac{T_e r}{T_l} Z' \left( \frac{\omega}{KV_l} \right), \quad (1)$$

where

$$V_i = (2T_i/M_i)^{1/2}, \quad K_e^2 = 4\pi n_e e^2 / T_e, \\ r = n_l / n_e = 1 - n_h / n_e,$$

the subscripts  $l$  and  $h$  are for light and heavier ions, respectively, and  $Z$  is the plasma dispersion function.<sup>5</sup> We took Maxwell distributions as the unperturbed distribution functions. The first term on the right-hand side of Eq. (1) comes from the electrons, the second term from the heavy ions, the third term from the light ions. The following results have been obtained by solving Eq. (1) numerically for  $\omega/K$  which has complex  $\omega$  and real  $K$  with the assumption that  $T_h = T_l = T_i$  and that  $K \ll K_e$  for the Ar-He plasma. When  $T_e/T_i > 20$ , as  $r$  increases from zero, the velocity of the principal argon mode, which is about  $[(T_e + 3T_i)/M_h]^{1/2}$  at  $r=0$ , increases continuously and finally at  $r=1$  it becomes  $[(T_e + 3T_i)/M_l]^{1/2}$ , which is the ion-acoustic velocity of helium-ion plasma. When  $T_e/T_i \leq 20$ , on the other hand, as  $r$  increases from zero, the phase veloc-

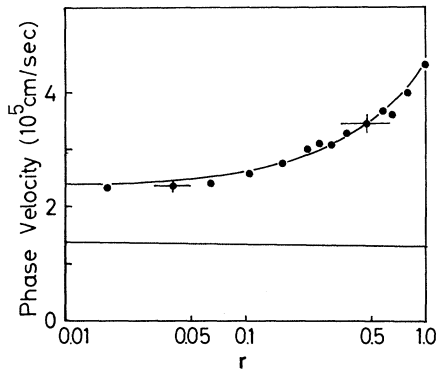


FIG. 3. Dependence of phase velocity on neon-ion concentration. The solid curves are calculated from Eq. (2) for  $T_e/T_i = 15$ .

ity of the argon mode decreases gradually. Finally, at the limit  $r = 1$  it becomes nearly equal to  $V_h$  which is the mean thermal velocity of argon ions. As  $r$  decreases from unity, the phase velocity of the helium ion-acoustic wave decreases and at the limit  $r = 0$  it is about  $V_l$ . The phase velocities of these two modes calculated from Eq. (1) are shown in Fig. 2 by the solid line for  $T_e/T_i = 10$  and by the dashed line for  $T_e/T_i = 15$ . Here  $T_e = 1.8$  eV which had been measured by the Langmuir probe when  $r \approx 0.5$ . Experimental results agree with theory within experimental errors.

Interferometer data for the Ar-Ne plasma did not show the interference pattern of two waves in the whole range of  $r$ . Only a single pulse was detected by the time-of-flight technique. The obtained ion-acoustic velocity of the Ar-Ne plasma is shown in Fig. 3 as a function of the neon-ion concentration. The electron temperature varied from 2.0 eV when  $r = 0$  to 3.6 eV when  $r = 1$ . Since  $T_i$  was 0.15 and 0.22 eV when  $r$  was 0 and 1, respectively, the ratio  $T_e/T_i$  was about 15 in the whole range of  $r$ .

We consider the following fluid dispersion relation obtained easily from the one-dimensional multispecies equations of motion and continuity and Poisson's equation:

$$K^2 = \frac{\omega_e^2}{(\omega/K)^2 - \frac{1}{2}V_e^2} + \frac{(1-r)\omega_h^2}{(\omega/K)^2 - \frac{3}{2}V_h^2} + \frac{r\omega_l^2}{(\omega/K)^2 - \frac{3}{2}V_l^2}, \quad (2)$$

where  $\omega_i^2 = 4\pi n_e e^2/M_i$ . For the Ar-Ne plasma,  $\omega/K$  has been obtained from Eq. (2) as a function of  $r$  with the assumption that  $K/K_e \ll 1$  and  $\omega/K \ll V_e$ . The result is shown by solid curves in Fig.

3. Here  $T_e/T_i = 15$  and the measured values of  $T_e$  have been used. The ion-acoustic velocity estimated from Eq. (1) is very close to the upper curve shown in Fig. 3. This velocity is nearly equal to  $\{(T_e + 3T_i)/M_f\}^{1/2}$ , where the effective mass  $M_f$  is given by  $1/M_f = r/M_l + (1-r)/M_h$ . From the results described above, it is concluded that only a single mode is seen to exist in the Ar-Ne plasma when  $T_e/T_i = 15$ . The lower branch in Fig. 3, which starts from  $(\frac{3}{2})^{1/2}V_l$  at  $r = 0$ , cannot be observed experimentally.

The phase velocities  $\omega/K$  obtained from Eq. (2) for the Ar-He plasma when  $T_e/T_i = 10$  to 15 are close to those calculated from Eq. (1). Therefore, the experimental results can be explained as follows by considering the fluid dispersion relation Eq. (2). In the case of the Ar-Ne plasma, since  $V_h < V_l \ll \omega/K$ , neon ions oscillate in a wave field in phase with argon ions and electrons. Consequently, the equivalent mass of the ions is equal to  $M_f$ ; in other words, the addition of a small amount of light ions increases the phase velocity of the wave. Next, we consider the physical difference between the upper and the lower modes in Fig. 2. As for the lower mode, the third term of the right-hand side of Eq. (2) is negative since  $(\frac{3}{2})^{1/2}V_h < \omega/K < (\frac{3}{2})^{1/2}V_l$ . It means that helium ions added to the argon plasma oscillate out of phase with the oscillating argon ions and electrons. Hence the phase velocity of this mode decreases by addition of light ions. As for the upper branch in Fig. 2, both kinds of ions oscillate in phase.

The results have important implications for the use of the waves as a diagnostic tool for measuring ion concentration. A possible other interesting application might be the heating of heavy ions by ion-acoustic turbulences driven by an electron drift or ion beam in the two-ion plasma. As we have seen above, the addition of light ions reduces the wave phase velocity of the heavy-ion mode and the number of heavy ions which interact with the wave increases. This may occur in the ion-acoustic wave which is considered to be excited by the field-aligned current and to play an important role in acceleration of ions in the auroral ionosphere which is composed of several kinds of ions.

<sup>1</sup>W. D. Jones, A. Lee, S. M. Gleman, and H. J. Doucet, Phys. Rev. Lett. **35**, 1349 (1975).

<sup>2</sup>B. D. Fried, R. B. White, and T. K. Samec, Phys. Fluids **14**, 2388 (1971).

<sup>3</sup>I. Alexeff, W. D. Jones, and D. Montgomery, *Phys. Rev. Lett.* **19**, 422 (1967).

<sup>4</sup>M. Nakamura, M. Ito, Y. Nakamura, and T. Itoh,

*Phys. Fluids* **18**, 651 (1975).

<sup>5</sup>B. D. Fried and S. D. Conte, *The Plasma Dispersion Function* (Academic, New York, 1961).

## Chemical Trends in Atomic Adsorption on Simple Metals

N. D. Lang and A. R. Williams

*IBM Thomas J. Watson Research Center, Yorktown Heights, New York 10598*

(Received 4 March 1976)

Essentially exact numerical solutions of the self-consistent atom-jellium model are used to show how the chemical concepts of electronegativity, shell-filling, and covalent or ionic bonding manifest themselves in the microscopic redistributions of charge and state density which accompany chemisorption. Realistic results are provided for chemisorbed Li, Cl, and Si, illustrating the three basic types of bonding—cationic, anionic, and covalent.

In the work reported here, the self-consistent atom-jellium model<sup>1</sup> is used to study the adsorption on a dense simple-metal surface of three atoms—Li, Si, and Cl—which are sufficiently different chemically that their binding to such a surface spans the phenomenology we expect to find in chemisorption on simple metals (when neither spin fluctuations nor permanent moments are important). This study is motivated by the conviction that we must abstract from our understanding of relatively simple systems, in which detailed analysis is possible, the concepts which will enable us to think effectively about more complex cases.

As an atom approaches a surface, those of its energy levels which are (or become) degenerate with the energy bands of the metal broaden into resonances, permitting nonintegral occupation. The final position of each resonance relative to the Fermi energy ( $E_F$ ), and therefore its occupation, result from the competition among the atom's desire to fill its valence shell, the intra-atomic Coulomb repulsion energy required to do so, and the electron affinity of the metal. The range of possible behavior is illustrated in Fig. 1. The  $2s$  resonance of Li lies primarily above<sup>2</sup>  $E_F$  and the  $3p$  resonance of Cl lies below  $E_F$ , providing clear examples of positive and negative ionic chemisorption. The direction of charge transfer is consistent with the electronegativities of Li, Cl, and an Al<sup>1</sup> surface. Filling the valence shell of Cl and emptying that of Li both involve only a single electron; to fill or empty that of Si would involve four electrons. The energetic cost of this results in the partial occupation of the Si

$3p$  resonance seen in Fig. 1, which has important implications for the electron density. The states in the lower-energy part of any resonance have greater amplitude in the bond region than those in the upper part.<sup>3</sup> For Si near its equilibrium separation, the scale of this amplitude difference is large and the preferential occupation of bonding states results in a clearly discernible covalent bond charge (see below).

The motivation for looking at electron densities is that they provide a spatially detailed picture of bonding which is independent of the analytical approach employed. Further, the existence of comprehensive analyses of electron densities in related molecular systems<sup>4</sup> makes it possible to compare the chemical trends in these extensively

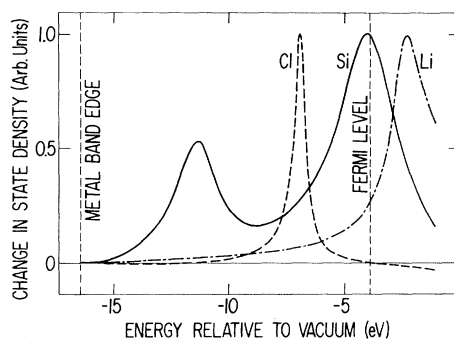


FIG. 1. Change in state density due to chemisorption (cf. Ref. 1). Curves correspond to positive-background-atom nucleus separations which minimize total energy [2.5 a.u. (Li), 2.3 a.u. (Si), 2.6 a.u. (Cl)]. Note that lower Si resonance corresponds to the  $3s$  level of the atom; for Cl, this is a discrete state below the band edge.